

Putting the Squeeze on Phase Separation

Carla Fernández-Rico, Tianqi Sai, Alba Sicher, Robert W. Style, and Eric R. Dufresne*

Cite This: *JACS Au* 2022, 2, 66–73

Read Online

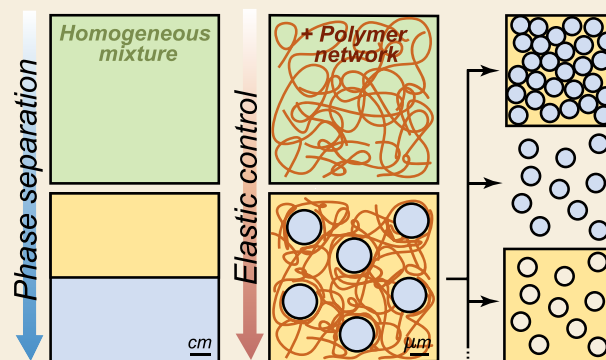
ACCESS |

Metrics & More

Article Recommendations

ABSTRACT: Phase separation is a ubiquitous process and finds applications in a variety of biological, organic, and inorganic systems. Nature has evolved the ability to control phase separation to both regulate cellular processes and make composite materials with outstanding mechanical and optical properties. Striking examples of the latter are the vibrant blue and green feathers of many bird species, which are thought to result from an exquisite control of the size and spatial correlations of their phase-separated microstructures. By contrast, it is much harder for material scientists to arrest and control phase separation in synthetic materials with such a high level of precision at these length scales. In this Perspective, we briefly review some established methods to control liquid–liquid phase separation processes and then highlight the emergence of a promising arrest method based on phase separation in an elastic polymer network. Finally, we discuss upcoming challenges and opportunities for fabricating microstructured materials via mechanically controlled phase separation.

KEYWORDS: phase separation, arrest, bird feathers, elasticity, polymer networks, microstructured materials



A. THE PROMISE AND CHALLENGE OF PHASE SEPARATION

Few physical processes in material science span the huge range of length scales accessed during phase separation. Consider the formation of a familiar drop of dew, condensing on a blade of grass on a cool summer morning. Starting from its critical radius, around a nanometer, it grows smoothly from the surrounding supersaturated air until it reaches its final gravity-limited size of about a millimeter. Condensation is just one example of a broad class of phase separation processes, where homogeneous mixtures of immiscible components separate into distinct phases to reach thermodynamic equilibrium (Figure 1A).¹

Phase separation can be triggered by a variety of stimuli, including temperature, composition, or activity changes.^{2–4} In homogeneous mixtures of fluids, phase separation takes place via nucleation and growth or via spinodal decomposition.⁵ These two classic demixing pathways entail very different morphologies consisting of a dispersion of discrete droplets (Figure 1A(i)) or a bicontinuous network formed by interconnected channels (Figure 1A(ii)). Because the interface between these biphasic structures costs energy, their microscopic features tend to vanish over time, with interfacial forces driving their coarsening into two macroscopic domains (Figure 1A(iii)).⁵

The transient nano- and microstructures formed during phase separation have been widely exploited by natural evolution and human ingenuity. For instance, living cells use

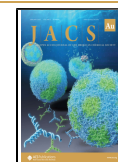
phase separation to structure the cytoplasm and regulate biological functions via the formation of protein-rich droplets.^{6–8} Humans have also harnessed phase separation during millenia for a variety of purposes. For example, the phase separation of gas within bread dough creates a solid foam, which improves bread's texture and digestibility.⁹

More recently, scientists have exploited phase separation to fabricate advanced functional materials with engineered microstructures. Some examples include the fabrication of metal alloys,^{10,11} colloidal particles,^{12–15} and porous materials.^{16–20} The central challenge in controlling the microstructure of phase-separated materials is to arrest their demixing at the desired length scale. In mixtures of fluids, this is not always an easy task, as classical liquid–liquid phase separation processes have no intrinsic mechanisms to overwhelm the ubiquitous influence of surface tension.

In this Perspective, we discuss the potential of using mechanical forces imposed by polymer matrixes to control liquid–liquid phase separation at the microscale. We begin by briefly reviewing some established methods to arrest demixing processes. Then, we draw inspiration from some natural

Received: October 7, 2021

Published: December 10, 2021



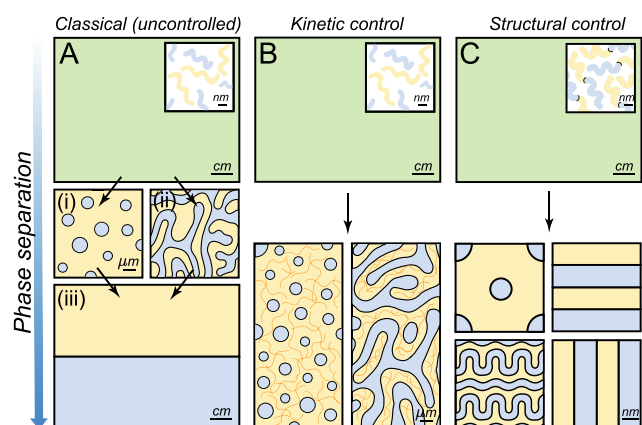


Figure 1. Liquid–liquid phase separation and some established methods to control it. (A) Classical (uncontrolled) phase separation of a homogeneous mixture where the two immiscible components (blue and yellow) demix by either (i) nucleation and growth or (ii) spinodal decomposition until they form (iii) two distinct macroscopic phases. (B) Kinetic control of phase separation by vitrification or cross-linking of one of the phases. (C) Structural control of phase separation by using block-*co*-polymers: the two immiscible components are chemically bound (inset), which introduces an internal length scale: a range of periodic structures are obtained.

examples which suggest that greater control of these processes is possible. Next, we focus on some recent studies exploring the impact of elastic polymer matrixes on phase separation, and finally, discuss the challenges and opportunities of elastically controlled phase separation methods.

B. ESTABLISHED APPROACHES TO ARREST LIQUID–LIQUID PHASE SEPARATION

Vitrification or gelation of one phase is a powerful approach to arrest liquid–liquid phase separation at the microscale (Figure 1B).^{16,21–23} For example, porous polymer membranes for filtration are made from a polymer solution where phase separation is triggered by a rapid thermal or solvent-composition quench.¹⁶ Phase separation arrests microscopically when the polymer-rich phase vitrifies, i.e. when it reaches a glassy state, due to the reduced mobility of the polymer chains. Using this kinetic approach, the final structure of the material can be tuned over multiple length scales, as it depends on the competition between the coarsening rate of the phase-separated domains and the quenching rate of the system.¹⁶ Similar glass-transition arrest processes are used to produce many other phase-separated materials, including colloidal gels,^{21,24} protein gels,²² and colloidal particles with several subdomains.^{23,25}

The cross-linking or polymerization of one component can also robustly arrest phase separation at microscopic scales.^{26–28} An example of this approach is the fabrication of polymer-dispersed liquid crystals, which are optically active composite materials, and are produced by cross-linking an epoxy-based polymer mixed with a liquid crystal mesogen.²⁶ As the cross-linking reaction proceeds, the mixture becomes unstable and liquid crystalline droplets form in the polymer phase. Eventually, when cross-linking rigidifies the polymer domains, further phase separation is arrested and the microstructure of the material is stabilized. Compared to the vitrification approach described above, cross-linking may be more attractive for producing homogeneously structured materials. This is

because the quenching of the system, i.e. its cross-linkage, is not limited by the diffusion of heat or mass throughout the system, but by the kinetics of the cross-linking reaction. As a result, the ultimate length scale of the material is determined by the kinetic competition of coarsening and cross-linking of the system.²⁷

The above strategies for controlling the structure of phase-separated materials are based on the kinetics of demixing. A major breakthrough in regulating this process came with the advent of block copolymers, whose structure introduces an intrinsic length scale into the system and confers thermodynamic stability to phase-separated structures at the nanoscale.^{29–33} In these systems, mixtures of polymers with a tendency to phase separate are linked by a covalent bond (inset Figure 1C). When demixing is triggered, the bonds between the different polymer blocks restrict their relative motion and hence oppose macroscopic phase separation. These constraints lead to the formation of highly ordered microscopic domains with dimensions comparable to the size of their macromolecular building blocks. Examples of such periodic structures include lamellar, hexagonal, and gyroid structures³⁴ (Figure 1C). Furthermore, with the development of brush-block copolymers, phase-separated materials with structural scales comparable to the wavelength of light, were also produced.^{35,36} Finally, while the applications of block-polymer materials have been typically limited to small sample volumes due to complex synthesis and sluggish assembly of these gigantic macromolecules,³⁷ recent works show their potential for the centimeter-scale production of photonic structures.³⁸

In summary, while beautifully ordered phase-separated materials can be produced through the precise structural control of their molecular building blocks, kinetic approaches to control phase separation work with simpler chemistries and access a wider range of length scales. Could systems with simpler molecular architectures also produce robustly ordered structures over a wide range of length scales? A look at nature suggests that they might be able to.

C. BIOINSPIRATION: PHOTONIC NANOSTRUCTURES IN FEATHERS

Bird feathers produce vivid colors (Figure 2A–C) through a variety of mechanisms.³⁹ For instance, noniridescent greens and blues are typically formed by the scattering of light from partially ordered structures made of β -keratin and air, as those shown in the electron microscopy images (Figure 2D–F).^{40,41} All of these structures have a well-defined length scale, which is observable as a ring in X-ray scattering measurements (Figure 2G–I). Most known examples of color-producing structures in bird feathers adopt two typical morphologies with short-ranged translation order. These are channel-like structures resembling arrested spinodal decomposition (Figure 2D) and dense packings of uniform spheres resembling arrested nucleation and growth (Figure 2E).⁴¹

The striking similarity of the birds' photonic structures to classical liquid–liquid phase separation morphologies suggest that these structures form through the phase separation of β -keratin proteins in the cytoplasm of their medullary cells.^{40,42} This hypothesis is supported by that fact that these nanostructures appear during keratinization, which is a process where cells undergo programmed cell death while over-expressing keratin. Ultimately, nearly all of the mass of the cell is replaced by solid keratin. At some point during this process,

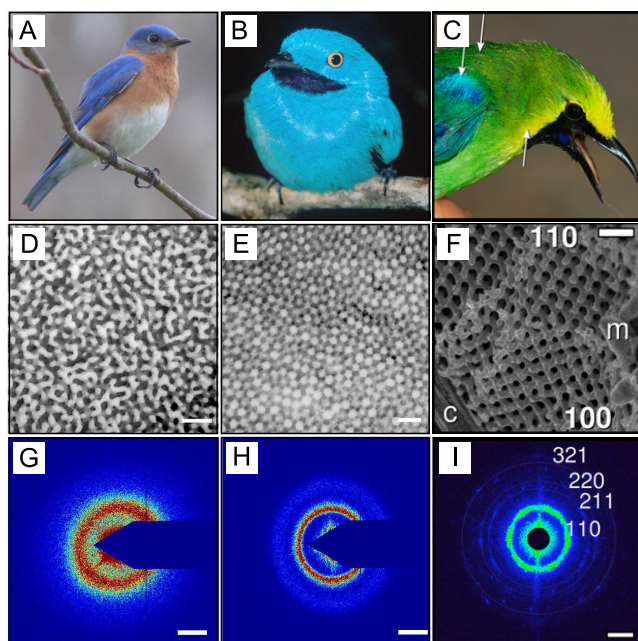


Figure 2. Examples of coloration in bird feathers by structures formed during arrested phase separation. (A–C) Pictures of (A) *Sialia sialis*, (B) *Cotinga maynana*, and (C) *C. cochinchinensis kinneari*. (D–F) Scanning electron microscopy images of the underlying structure: (D) channel type, (E) sphere-type and (F) gyroid-type β -keratin and air nanostructure (G–I) X-ray scattering plots. Scale bars are (D–F) 500 nm and (G–I) 0.025 nm^{-1} . Reproduced with permission from ref 40, Copyright 2009 Royal Society of Chemistry, and from ref 45, Copyright 2021 National Academy of Sciences.

the concentration of cytoplasmic keratin necessarily exceeds its solubility limit, driving phase separation. A similar process occurs in mammalian skin and hair, but with the protein α -keratin. In color-producing medullary cells, an unknown mechanism arrests the phase separation to create the well-defined nanostructures pictured in Figure 2D–E. Arrest could be driven by a variety of factors, including the formation of disulfide cross-links between β -keratin filaments, or elastic stresses, as discussed in the next Section.

Recent developments in cellular and molecular biology^{6–8,43,44} show that, indeed, cells can have exquisite control of phase separation for compartmentalization and control of chemical reactions in the cytoplasm.^{6–8} Nonetheless, the resulting phase-separated protein droplets in cells typically appear at much lower volume fractions than those observed in, for instance, Figure 2E (see, e.g., ref 6). Birds appear to be uniquely capable of precisely assembling highly packed and uniform nanostructures, through arrested phase separation.⁴⁰ At the moment, we are not aware of any synthetic process that can arrest phase separation at this length scale with such flexibility or precision.

Birds' repertoire of phase-separated morphologies extends beyond the spherical and spinodal structures expected from classic liquid–liquid phase separation. Saranathan and coworkers recently discovered that the medullary cells of blue-winged leafbirds can also produce vibrant blue and green colors by light scattering from crystalline nanostructures (Figure 2C).⁴⁵ These structures have an exotic structure, called the single network gyroid (Figure 2F and I), which is characterized by a cubic lattice constructed from valence-three subunits.⁴⁶ While interpenetrating gyroids can be experimen-

tally obtained from the self-assembly of triblock copolymers,⁴⁷ their lattice spacing is set by the size of their constituent macromolecules, which does not appear to be the case in bird feathers.³⁷ A direct path to assemble single gyroid structures therefore still remains an exciting experimental challenge.

D. ELASTIC CONTROL OF PHASE SEPARATION

Birds' ability to precisely regulate phase separation to produce photonic microstructures is impressive. This begs the question: "How do they do it?". Here, we explore the hypothesis that elastic stresses could play a major role in regulating phase separation processes in cells. Groundbreaking work by Tanaka and colleagues showed that viscoelastic stresses can have a significant impact on the morphology of phase separating systems,⁴⁸ specifically favoring the formation of network structures, like those observed recently in ref 49. In the meantime, it has become clear that the cytoplasm has complex rheology, with elastic contributions from several factors, including the cytoskeleton.^{50,51}

To experimentally explore the impact of elastic stresses on phase separation processes, we developed a synthetic system based on liquid droplets condensing in a preformed polymeric network.^{52–54} This simple system consists of a silicone gel, which is immersed in a bath of fluorinated oil at an elevated temperature (Figure 3A). Once the gel is homogeneously saturated with oil, it is cooled to reduce its solubility and induce phase separation (Figure 3A). This process produces remarkably uniform micrometer-sized oil droplets (Figure 3B), whose size and number density are correlated to the network stiffness (i.e., Young's modulus, E).⁵² As shown in Figure 3C, stiffer networks produce smaller droplets at a higher number density. Note that the stiffness of the network is controlled by its cross-linking density.

The governing role of mechanical forces in phase separation was further clarified by triggering phase separation in stretched networks.⁵⁵ In those experiments, condensed droplets were not only uniform in size, but grew with a self-similar elliptical shape, which reflected the underlying state of stress of the network (inset Figure 3B). These results show convincingly that continuum mechanical properties of the host phase can regulate the size and shape of dilute phase-separated structures. Elastic stresses were also found to drive ripening of the oil droplets along stiffness gradients.⁵⁴ Furthermore, the production of uniform phase-separated droplets in polymer networks was shown to be generic. This was demonstrated by using both physically and chemically cross-linked hydrogels, where phase separation was driven by changes in solvent.⁵²

In our view, interesting results emerge when the driving forces of condensation and the mechanics of the network become strongly coupled. From a thermodynamic perspective, the pressure exerted by a droplet during condensation is limited to a maximum value, P_{cond} (Figure 3D), set by the second law of thermodynamics.¹ When the saturation condensation is sufficiently dilute,

$$P_{\text{cond}} = n_L k_B T \ln \left(\frac{n}{n_{\text{sat}}} \right) \quad (1)$$

Here, n is the number density of the condensing molecule in the polymer network, and n_L and n_{sat} are the equilibrium concentrations of the condensing molecule in the droplet and network phases. In the simplest model of a polymer network, its mechanical properties are captured by its Young's modulus,

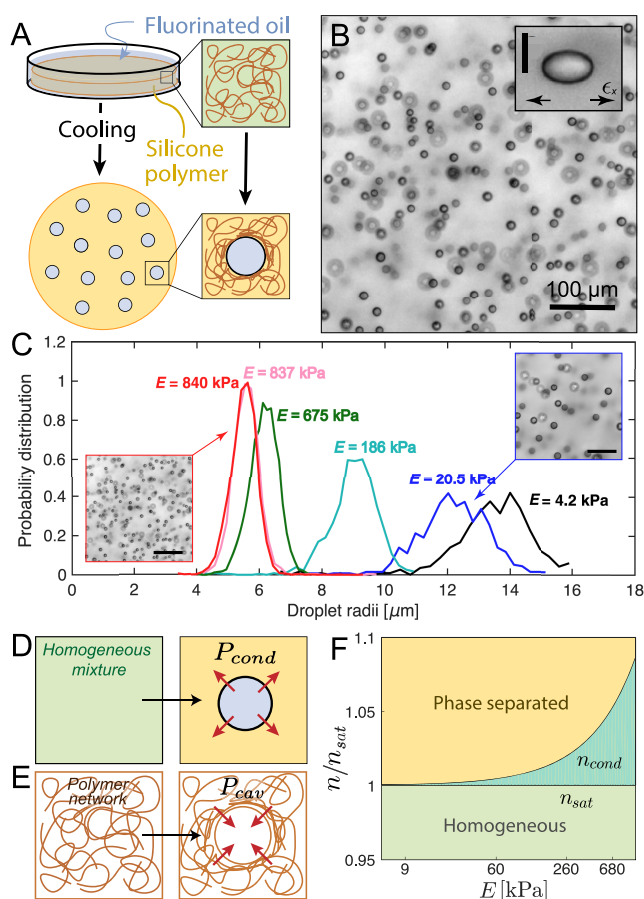


Figure 3. Elastic control of phase separation. (A) Schematic diagram of temperature-induced nucleation and growth of fluorinated oil droplets in silicone polymer networks. (B) Bright-field microscopy image of the typical oil droplets formed in the silicone gels.⁵² Inset shows how network stresses cause the droplets to grow with elliptical shapes.⁵⁵ The scale bar is 10 μm. (C) Typical droplet distributions in different gel stiffnesses, E . Microscopy images shown the evolution of the droplets' number density with E .⁵² Scale bars are 80 μm. (D) Schematic of the condensation of a single droplet, exerting a condensation pressure, P_{cond} into the continuous phase. (E) Schematic of the creation of a spherical cavity on a polymer matrix. The opposing pressure exerted by the network is the cavitation pressure P_{cav} . (F) Phase diagram of the stability of a homogeneous mixture depending on the supersaturation of the mixture and the stiffness of the network.⁵⁴ Reproduced with permission from ref 52, Copyright 2018 American Physical Society, from ref 54, Copyright 2020 Nature Research, and from ref 55, Copyright 2020 American Association for the Advancement of Science.

E . In our system, the droplets exclude the network as they grow.⁵⁵ According to the classic theory of elastic cavitation,^{56,57} the minimum pressure needed to freely expand an isolated spherical cavity in a polymer network, P_{cav} is about equal to E . This means that droplet nucleation in a polymer network is only allowed when $P_{\text{cond}} > P_{\text{cav}}$ (Figure 3E). By equating these two pressures, we can identify the minimal concentration of fluorinated oil needed for condensation in an elastic network, n_{cond} , which shows an exponential dependence with E .⁵⁴ This coupling between the thermodynamics of condensation and the network elasticity is illustrated in the phase diagram in Figure 3F. Here, the phase boundary separating the single-phase (green) and two-phase (yellow) regions is no longer a flat line but it exponentially increases with the elastic modulus

of the network (n_{cond} in Figure 3F). In simpler terms, elastic stresses are able to stabilize supersaturated mixtures against phase separation (dark green region in Figure 3F).⁵⁴ When the system is driven far past the phase boundary, i.e. $P_{\text{cond}} > P_{\text{cav}}$, the network provides no significant resistance to condensation and droplets grow freely.⁵⁴ However, as condensation proceeds, n and P_{cond} decrease. Eventually, $P_{\text{cond}} \approx P_{\text{cav}}$, and further growth is arrested by elastic stresses in the network.

A central outstanding question is what determines the final size of the droplets. While there is a strong correlation between the droplet size and the network's stiffness, the supersaturation level and cooling rate used during the phase separation process also affects the droplet size.⁵² The later suggests that the final droplet size is not only dependent on the coupling between elasticity and thermodynamics, but also on kinetic aspects of the phase separation process. Furthermore, recent experiments have shown that gels with the same E , but slightly different chemical compositions, can produce droplets with different sizes.⁵³ This implies that other factors, such as the microstructure of the network and its nonlinear mechanical properties could also play a role. Related theoretical studies have shed some important light on these systems,^{58–62} which will be discussed in more detail in the next section.

Our studies on the fluorinated oil/silicone system may be closely related to earlier work on the volumetric phase separation in swollen gels.^{63–66} In that case, a swollen polymer network wants to phase separate from the solvent phase, but the solvent is inhibited from being expelled out of the gel's surface. This can be triggered by a wide variety of stimuli, including temperature, pH or light, and results in phase separation into network-rich and network-poor phases.^{63–66} Here again, the separation process is again governed by a balance between network elasticity and the usual entropic and enthalpic effects that control phase separation.⁶⁷ Recent work on polyampholyte hydrogels has also shown that this approach can be used to produce microstructures with a well-defined length scale,^{49,68} which are capable of producing a structural color.

The central message unifying these results is that elasticity provides an additional dimension to control phase separation processes. Compared to the classical methods presented in Section B, this approach produces materials with remarkably uniform phase-separated domains, whose dimensions are distinct from the size of their supramolecular building blocks. These are two essential aspects of the photonic nanostructures found in bird feathers, hence suggesting that elasticity may indeed be involved in the regulation of their formation.

E. CHALLENGES AND OPPORTUNITIES

In the previous section, we showed that mechanical stresses can control the size, number, and even the shape of micrometer-sized droplets condensing in a polymer network. While we have also discussed how this approach has strong connections with the phase-separation process in bird feathers, here, we would like to speculate about how these findings could be built upon to develop useful materials. An overview of these future directions is shown in Figure 4.

1. Tuning Droplet Size over a Broad Range

Different applications require composite materials to be structured at different length scales. While photonic structures are characterized by features on the order of hundreds of nanometers,⁶⁹ membranes require pore sizes that can range

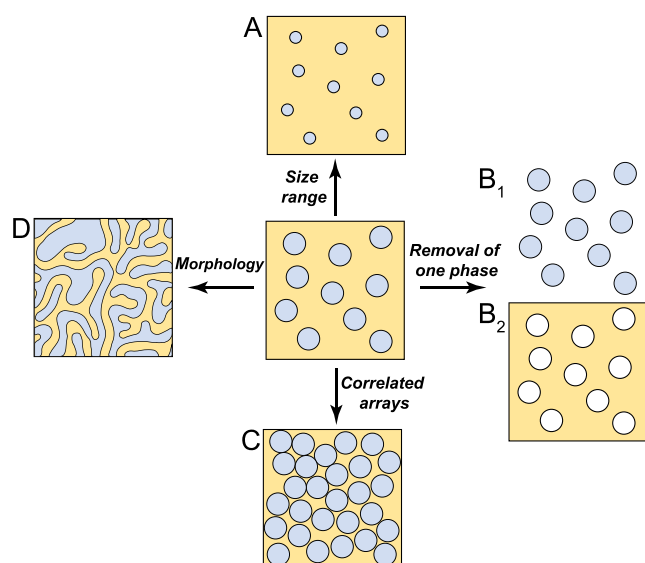


Figure 4. Potential developments in the fabrication of microstructured materials through phase separation in elastic media. (A) Access to a wider range of droplet sizes. (B) Fabrication of (B₁) standing-free liquid or polymer particles and (B₂) porous materials. (C) Assembly of structures with higher packing fractions showing structural correlations. (D) Fabrication of interconnected channel structures via spinodal decomposition.

from a few nanometers up to the micrometer scale and above.⁷⁰ To address such needs, we must be able to accurately tune the size of structures produced by elastically controlled phase separation over a broader range (Figure 4A), ideally several orders of magnitude.

While our current system is limited to produce droplets of several micrometers,⁵² there are a variety of approaches that could expand the range of available structural length scales. Most obviously, stiffer polymer networks with $E \sim \text{MPa}$ could be used to produce smaller droplets. However, this will ultimately be limited by the fact that the supersaturation necessary to grow droplets increases exponentially with stiffness (Figure 3F). Alternatively, the quenching of the system could also be made faster. The current thermal quenching approach is an inherently slow process, as it relies on the diffusivity of heat through the material. We expect that much faster quenching could be achieved with pressure. Finally, seeded nucleation could effectively increase the number of droplets, thereby reducing their size.

Recent theoretical works have suggested that other parameters could impact droplet size.^{58–62} For example, thermodynamics should favor the formation of smaller droplets when these have lower surface energies.⁶² This could be achieved by the addition of surfactants, or by using macromolecular condensing species, such as a phase separating protein system.^{43,71} The mesh size of the confining network has also been predicted to play a key role.⁶² This length scale could be tuned while maintaining stiffness of the network through the use of semiflexible polymers.⁷² Finally, nonlinear rheology should also play an important role.⁶² In fact, strain-stiffening materials, like many biopolymers, have been also predicted to thermodynamically arrest droplets at much smaller sizes, as the work to grow droplets increases significantly with their size.⁵⁸

2. Selective Removal of One Phase

Elastic phase separation provides a novel route to fabricate uniform droplets. This simple physical process should, in principle, be applicable to a wide range of chemistries. The only requirement is that the material forming the droplets should be partially miscible in the selected elastic matrix. Interestingly, if one chooses a degradable polymer as the elastic network, uniform droplets, or even particles (if droplets are polymerized), could be produced after the removal of the elastic confinement (Figure 4B₁). Yield stress gels⁷³ and degradable hydrogels⁷⁴ seem like attractive choices for this procedure. Conversely, the removal of the phase-separated domains, could lead to the production of porous materials with well-defined structure (Figure 4B₂).

Indeed, the polymerization of phase-separated domains could be a powerful route to produce monodisperse particles whose chemistries are not amenable to traditional colloidal syntheses. These could include poly(lactic-co-glycolic) acid or other biodegradable polymers targeting drug delivery applications, whose currently colloidal production yields polydisperse particles.⁷⁵ Finally, it is important to note that even without extraction from the network, the polymerization of the phase-separated droplets is attractive as it would stabilize microstructures against elastic ripening and evaporation^{53,54} and hence form permanently microstructured materials.

3. Correlated Arrays

The properties of composite materials depend not only on the size of inclusions, but also their spatial organization. For example, photonic nanostructures require strong structural correlations, as found in Figure 2. Experiments and theory of elastically controlled phase separation have so far been limited to the dilute limit, where phase-separated domains are essentially independent. We generically expect structural correlations to arise as the concentration of phase-separated domains increases (Figure 4C), in analogy to concentrated suspensions of monodisperse colloids which spontaneously self-assemble into (partially) ordered phases.^{76,77}

Experimentally, an essential first step is to identify systems with large changes in solubility with modest changes in temperature or pressure. This could be achieved, for example, by polymerizing a soluble monomer to precipitate out polymeric inclusions⁷⁸ or by using stimuli-responsive polymer networks.⁷⁹

4. Bicontinuous Networks

The above discussion has focused on isolated domains that form via nucleation and growth. However, it should also be possible to form bicontinuous network structures (Figure 4D), such as those shown in the photonic bird feathers in Figure 2D and F. Such structures are typically achieved through spinodal decomposition and have found a range of other applications such as catalysis, fuel cells, batteries, and membranes, where a large surface area is required.¹⁷ While the impact of viscoelasticity has been extensively studied,⁴⁸ the impact of elasticity on spinodal decomposition still remains unexplored. A recent theoretical work introduced a mean field theory of phase separation in an elastic network to calculate the resulting phase diagram of the system. Interestingly, the phase diagram showed an unusual geometry, where the critical point was replaced by a critical line. This suggests that an appropriate elastic network might facilitate the experimental access to the spinodal regime.⁵⁹ One exciting possibility is that long-range elastic forces could help organizing spinodal decom-

position, possibly creating highly ordered network structures like those observed in Figure 2F.

F. CONCLUSIONS

In the last decades, applications of phase separation to fabricate nano- and microstructured materials have advanced dramatically. However, a close look at the natural world suggest there is still significant room for improvement. Here, we have highlighted some emerging approaches to control phase separation based on mechanical constraints, and discussed potential links with the phase-separation processes observed in bird feathers. Finally, we have outlined a number of challenges and opportunities on the horizon for understanding and exploiting elastically controlled demixing processes. Whether phase separation in elastic matrixes is an effective route to produce functional materials remains an open question, but recent results suggest a number of promising avenues for exploration.

AUTHOR INFORMATION

Corresponding Author

Eric R. Dufresne – Department of Materials, ETH Zürich, 8093 Zurich, Switzerland; orcid.org/0000-0002-3091-5039; Email: eric.dufresne@mat.ethz.ch

Authors

Carla Fernández-Rico – Department of Materials, ETH Zürich, 8093 Zurich, Switzerland; orcid.org/0000-0002-9472-1073

Tianqi Sai – Department of Materials, ETH Zürich, 8093 Zurich, Switzerland

Alba Sicher – Department of Materials, ETH Zürich, 8093 Zurich, Switzerland; orcid.org/0000-0002-6529-6186

Robert W. Style – Department of Materials, ETH Zürich, 8093 Zurich, Switzerland; orcid.org/0000-0001-5305-7658

Complete contact information is available at: <https://pubs.acs.org/10.1021/jacsau.1c00443>

Notes

The authors declare no competing financial interest.

ACKNOWLEDGMENTS

We acknowledge funding from the Swiss National Science Foundation NCCR for Bioinspired Materials. We thank Pierre Ronceray for useful discussions and Charlotta Lorenz for feedback on the manuscript.

REFERENCES

- (1) Gibbs, J. W. On the equilibrium of heterogeneous substances. *Transactions of the Connecticut Academy of Arts and Sciences* **1879**, *3*, 108.
- (2) Guillen, G. R.; Pan, Y.; Li, M.; Hoek, E. M. V. Preparation and Characterization of Membranes Formed by Nonsolvent Induced Phase Separation: A Review. *Ind. Eng. Chem. Res.* **2011**, *50*, 3798–3817.
- (3) Lloyd, D. R.; Kim, S. S.; Kinzer, K. E. Microporous membrane formation via thermally-induced phase separation. II. Liquid–liquid phase separation. *J. Membr. Sci.* **1991**, *64*, 1–11.
- (4) Fily, Y.; Marchetti, M. C. Athermal phase separation of self-propelled particles with no alignment. *Phys. Rev. Lett.* **2012**, *108*, 235–702.

- (5) Jones, R. A. L. *Soft condensed matter*; Oxford University Press, 2002; Vol. 6.
- (6) Brangwynne, C. P.; Eckmann, C. R.; Courson, D. S.; Rybarska, A.; Hoege, C.; Gharakhani, J.; Jülicher, F.; Hyman, A. A. Germline P Granules Are Liquid Droplets That Localize by Controlled Dissolution/Condensation. *Science* **2009**, *324*, 1729–1732.
- (7) Feric, M.; Vaidya, N.; Harmon, T. S.; Mitrea, D. M.; Zhu, L.; Richardson, T. M.; Kriwacki, R. W.; Pappu, R. V.; Brangwynne, C. P. Coexisting Liquid Phases Underlie Nucleolar Subcompartments. *Cell* **2016**, *165*, 1686–1697.
- (8) Banani, S. F.; Lee, H. O.; Hyman, A. A.; Rosen, M. K. Biomolecular condensates: organizers of cellular biochemistry. *Nat. Rev. Mol. Cell Biol.* **2017**, *18*, 285–298.
- (9) McGee, H. *On food and cooking: the science and lore of the kitchen*; Simon and Schuster, 2007.
- (10) Ardell, A. J. Precipitation hardening. *Metall. Trans. A* **1985**, *16*, 2131–2165.
- (11) Smith, T. M.; Esser, B. D.; Antolin, N.; Carlsson, A.; Williams, R. E. A.; Wessman, A.; Hanlon, T.; Fraser, H. L.; Windl, W.; McComb, D. W.; Mills, M. J. Phase transformation strengthening of high-temperature superalloys. *Nat. Commun.* **2016**, *7*, 13434.
- (12) Tseng, C.; Lu, Y.; El-Aasser, M.; Vanderhoff, J. Uniform polymer particles by dispersion polymerization in alcohol. *J. Polym. Sci., Part A: Polym. Chem.* **1986**, *24*, 2995–3007.
- (13) Sheu, H.; El-Aasser, M.; Vanderhoff, J. Phase separation in polystyrene latex interpenetrating polymer networks. *J. Polym. Sci., Part A: Polym. Chem.* **1990**, *28*, 629–651.
- (14) Kegel, W. K. Tuning particle geometry of chemically anisotropic dumbbell-shaped colloids. *J. Colloid Interface Sci.* **2017**, *490*, 462–477.
- (15) Moerman, P. G.; Hohenberg, P. C.; Vanden-Eijnden, E.; Bruijic, J. Emulsion patterns in the wake of a liquid-liquid phase separation front. *Proc. Natl. Acad. Sci. U. S. A.* **2018**, *115*, 3599–3604.
- (16) Wienk, I.; Boom, R.; Beerlage, M.; Bulte, A.; Smolders, C.; Strathmann, H. Recent advances in the formation of phase inversion membranes made from amorphous or semi-crystalline polymers. *J. Membr. Sci.* **1996**, *113*, 361–371.
- (17) Liu, X.; Ma, P. X. Phase separation, pore structure, and properties of nanofibrous gelatin scaffolds. *Biomaterials* **2009**, *30*, 4094–4103.
- (18) Xue, L.; Zhang, J.; Han, Y. Phase separation induced ordered patterns in thin polymer blend films. *Prog. Polym. Sci.* **2012**, *37*, 564–594.
- (19) Nakanishi, K.; Tanaka, N. Sol–Gel with Phase Separation. Hierarchically Porous Materials Optimized for High-Performance Liquid Chromatography Separations. *Acc. Chem. Res.* **2007**, *40*, 863–873.
- (20) Wang, D. M. Recent advances in preparation and morphology control of polymeric membranes formed by nonsolvent induced phase separation. *Current Opinion in Chemical Engineering* **2013**, *2*, 229–237.
- (21) Manley, S.; Wyss, H.; Miyazaki, K.; Conrad, J.; Trappe, V.; Kaufman, L.; Reichman, D.; Weitz, D. Glasslike arrest in spinodal decomposition as a route to colloidal gelation. *Phys. Rev. Lett.* **2005**, *95*, 238–302.
- (22) Cardinaux, F.; Gibaud, T.; Stradner, A.; Schurtenberger, P. Interplay between spinodal decomposition and glass formation in proteins exhibiting short-range attractions. *Phys. Rev. Lett.* **2007**, *99*, 118301.
- (23) Sosa, C.; Lee, V. E.; Grundy, L. S.; Burroughs, M. J.; Liu, R.; Prud'homme, R. K.; Priestley, R. D. Combining precipitation and vitrification to control the number of surface patches on polymer nanocolloids. *Langmuir* **2017**, *33*, 5835–5842.
- (24) Lu, P. J.; Zaccarelli, E.; Ciulla, F.; Schofield, A. B.; Sciortino, F.; Weitz, D. A. Gelation of particles with short-range attraction. *Nature* **2008**, *453*, 499–503.
- (25) Liu, J. X.; Bizmark, N.; Scott, D. M.; Register, R. A.; Haataja, M. P.; Datta, S. S.; Arnold, C. B.; Priestley, R. D. Evolution of Polymer

Colloid Structure During Precipitation and Phase Separation. *JACS Au* **2021**, *1*, 936–944.

(26) Doane, J.; Vaz, N.; Wu, B.-G.; Žumer, S. Field controlled light scattering from nematic microdroplets. *Appl. Phys. Lett.* **1986**, *48*, 269–271.

(27) Chan, P. K.; Rey, A. D. Polymerization-induced phase separation. I. Droplet size selection mechanism. *Macromolecules* **1996**, *29*, 8934–8941.

(28) Moore, D. G.; Barbera, L.; Masania, K.; Studart, A. R. Three-dimensional printing of multicomponent glasses using phase-separating resins. *Nat. Mater.* **2020**, *19*, 212–217.

(29) de Gennes, P.-G. Effect of cross-links on a mixture of polymers. *J. Phys., Lett.* **1979**, *40*, 69–72.

(30) Park, M.; Harrison, C.; Chaikin, P. M.; Register, R. A.; Adamson, D. H. Block copolymer lithography: periodic arrays of ~1011 holes in 1 square centimeter. *Science* **1997**, *276*, 1401–1404.

(31) Tang, C.; Lennon, E. M.; Fredrickson, G. H.; Kramer, E. J.; Hawker, C. J. Evolution of block copolymer lithography to highly ordered square arrays. *Science* **2008**, *322*, 429–432.

(32) Chen, X. C.; Li, H. M.; Fang, F.; Wu, Y. W.; Wang, M.; Ma, G. B.; Ma, Y. Q.; Shu, D. J.; Peng, R. W. Confinement-induced ordering in dewetting and phase separation of polymer blend films. *Adv. Mater.* **2012**, *24*, 2637–2641.

(33) Bates, F. S. Polymer-Polymer Phase Behavior. *Science* **1991**, *251*, 898–905.

(34) Darling, S. Directing the self-assembly of block copolymers. *Prog. Polym. Sci.* **2007**, *32*, 1152–1204.

(35) Sveinbjörnsson, B. R.; Weitekamp, R. A.; Miyake, G. M.; Xia, Y.; Atwater, H. A.; Grubbs, R. H. Rapid self-assembly of brush block copolymers to photonic crystals. *Proc. Natl. Acad. Sci. U. S. A.* **2012**, *109*, 14332–14336.

(36) Wang, Z.; Chan, C. L. C.; Zhao, T. H.; Parker, R. M.; Vignolini, S. Recent Advances in Block Copolymer Self-Assembly for the Fabrication of Photonic Films and Pigments. *Adv. Opt. Mater.* **2021**, *9*, 2100519.

(37) Bates, C. M.; Bates, F. S. 50th Anniversary Perspective: Block Polymers— Pure Potential. *Macromolecules* **2017**, *50*, 3–22.

(38) Patel, B. B.; Walsh, D. J.; Kim, D. H.; Kwok, J.; Lee, B.; Guirronnet, D.; Diao, Y. Tunable structural color of bottlebrush block copolymers through direct-write 3D printing from solution. *Science Advances* **2020**, *6*, No. eaaz7202.

(39) Hill, G. E.; McGraw, K. J., Eds. *Bird coloration: mechanisms and measurements*; Harvard University Press; 2006; Vol. 1.

(40) Dufresne, E. R.; Noh, H.; Saranathan, V.; Mochrie, S. G.; Cao, H.; Prum, R. O. Self-assembly of amorphous biophotonic nanostructures by phase separation. *Soft Matter* **2009**, *5*, 1792–1795.

(41) Saranathan, V.; Forster, J. D.; Noh, H.; Liew, S.-F.; Mochrie, S. G.; Cao, H.; Dufresne, E. R.; Prum, R. O. Structure and optical function of amorphous photonic nanostructures from avian feather barbs: a comparative small angle X-ray scattering (SAXS) analysis of 230 bird species. *J. R. Soc., Interface* **2012**, *9*, 2563–2580.

(42) Prum, R. O.; Dufresne, E. R.; Quinn, T.; Waters, K. Development of colour-producing β -keratin nanostructures in avian feather barbs. *J. R. Soc., Interface* **2009**, *6*, S253–S265.

(43) Shin, Y.; Brangwynne, C. P. Liquid phase condensation in cell physiology and disease. *Science* **2017**, *357*. DOI: 10.1126/science.aaf4382

(44) Bracha, D.; Walls, M. T.; Wei, M.-T.; Zhu, L.; Kurian, M.; Avalos, J. L.; Toettcher, J. E.; Brangwynne, C. P. Mapping Local and Global Liquid Phase Behavior in Living Cells Using Photo-Oligomerizable Seeds. *Cell* **2018**, *175*, 1467–1480.

(45) Saranathan, V.; Narayanan, S.; Sandy, A.; Dufresne, E. R.; Prum, R. O. Evolution of single gyroid photonic crystals in bird feathers. *Proc. Natl. Acad. Sci. U. S. A.* **2021**, *118*, No. e2101357118.

(46) Saranathan, V.; Osuji, C. O.; Mochrie, S. G. J.; Noh, H.; Narayanan, S.; Sandy, A.; Dufresne, E. R.; Prum, R. O. Structure, function, and self-assembly of single network gyroid (I4132) photonic crystals in butterfly wing scales. *Proc. Natl. Acad. Sci. U. S. A.* **2010**, *107*, 11676–11681.

(47) Dolan, J. A.; Wilts, B. D.; Vignolini, S.; Baumberg, J. J.; Steiner, U.; Wilkinson, T. D. Optical Properties of Gyroid Structured Materials: From Photonic Crystals to Metamaterials. *Adv. Opt. Mater.* **2015**, *3*, 12–32.

(48) Tanaka, H. Viscoelastic phase separation. *J. Phys.: Condens. Matter* **2000**, *12*, R207.

(49) Cui, K.; Ye, Y. N.; Sun, T. L.; Yu, C.; Li, X.; Kurokawa, T.; Gong, J. P. Phase Separation Behavior in Tough and Self-Healing Polyampholyte Hydrogels. *Macromolecules* **2020**, *53*, 5116–5126.

(50) Kasza, K. E.; Rowat, A. C.; Liu, J.; Angelini, T. E.; Brangwynne, C. P.; Koenderink, G. H.; Weitz, D. A. The cell as a material. *Curr. Opin. Cell Biol.* **2007**, *19*, 101–107.

(51) Wiegand, T.; Hyman, A. A. Drops and fibers - how biomolecular condensates and cytoskeletal filaments influence each other. *Emerging topics in life sciences* **2020**, *4*, 247–261.

(52) Style, R. W.; Sai, T.; Fanelli, N.; Ijavi, M.; Smith-Mannschott, K.; Xu, Q.; Wilen, L. A.; Dufresne, E. R. Liquid-liquid phase separation in an elastic network. *Phys. Rev. X* **2018**, *8*, 011–028.

(53) Rosowski, K.; Vidal-Henriquez, E.; Zwicker, D.; Style, R.; Dufresne, E. Elastic stresses reverse Ostwald ripening. *Soft Matter* **2020**, *16*, 5892.

(54) Rosowski, K. A.; Sai, T.; Vidal-Henriquez, E.; Zwicker, D.; Style, R. W.; Dufresne, E. R. Elastic ripening and inhibition of liquid-liquid phase separation. *Nat. Phys.* **2020**, *16*, 422–425.

(55) Kim, J. Y.; Liu, Z.; Weon, B. M.; Cohen, T.; Hui, C.-Y.; Dufresne, E. R.; Style, R. W. Extreme cavity expansion in soft solids: Damage without fracture. *Science advances* **2020**, *6*, No. eaaz0418.

(56) Gent, A.; Lindley, P. Internal rupture of bonded rubber cylinders in tension. *Rubber Chem. Technol.* **1961**, *34*, 925.

(57) Zimmerlin, J. A.; Sanabria-DeLong, N.; Tew, G. N.; Crosby, A. J. Cavitation rheology for soft materials. *Soft Matter* **2007**, *3*, 763–767.

(58) Kothari, M.; Cohen, T. Effect of elasticity on phase separation in heterogeneous systems. *J. Mech. Phys. Solids* **2020**, *145*, 104153.

(59) Wei, X.; Zhou, J.; Wang, Y.; Meng, F. Modeling elastically mediated liquid-liquid phase separation. *Phys. Rev. Lett.* **2020**, *125*, 268001.

(60) Vidal-Henriquez, E.; Zwicker, D. Cavitation controls droplet sizes in elastic media. *Proc. Natl. Acad. Sci. U. S. A.* **2021**, *118*, No. e2102014118.

(61) Zhang, Y.; Lee, D. S.; Meir, Y.; Brangwynne, C. P.; Wingreen, N. S. Mechanical frustration of phase separation in the cell nucleus by chromatin. *Phys. Rev. Lett.* **2021**, *126*, 258102.

(62) Ronceray, P.; Mao, S.; Košmrlj, A.; Haataja, M. P. Liquid demixing in elastic networks: cavitation, permeation, or size selection? *arXiv* **2021**, Submitted on 4 Feb 2021, preprint arXiv:2102.02787.

(63) Takeshita, H.; Kanaya, T.; Nishida, K.; Kaji, K. Spinodal decomposition and syneresis of PVA gel. *Macromolecules* **2001**, *34*, 7894–7898.

(64) Onuki, A.; Puri, S. Spinodal decomposition in gels. *Phys. Rev. E: Stat. Phys., Plasmas, Fluids, Relat. Interdiscip. Top.* **1999**, *59*, R1331.

(65) Sekimoto, K.; Suematsu, N.; Kawasaki, K. Sponglike domain structure in a two-dimensional model gel undergoing volume-phase transition. *Phys. Rev. A: At., Mol., Opt. Phys.* **1989**, *39*, 4912.

(66) Shibayama, M.; Tanaka, T. Volume phase transition and related phenomena of polymer gels. *Adv. Polym. Sci.* **1993**, *109*, 1–62.

(67) Onuki, A. Theory of phase transition in polymer gels. *Adv. Polym. Sci.* **1993**, *109*, 63–121.

(68) Li, X.; Cui, K.; Kurokawa, T.; Ye, Y. N.; Sun, T. L.; Yu, C.; Creton, C.; Gong, J. P. Effect of mesoscale phase contrast on fatigue-delaying behavior of self-healing hydrogels. *Science advances* **2021**, *7*, No. eaabe8210.

(69) Vukusic, P.; Sambles, J. R. Photonic structures in biology. *Nature* **2003**, *424*, 852–855.

(70) Baig, M. I.; Durmaz, E. N.; Willott, J. D.; de Vos, W. M. Sustainable membrane production through polyelectrolyte complexation induced aqueous phase separation. *Adv. Funct. Mater.* **2020**, *30*, 1907344.

- (71) Ijavi, M.; Style, R. W.; Emmanouilidis, L.; Kumar, A.; Meier, S. M.; Torzynski, A. L.; Allain, F. H.; Barral, Y.; Steinmetz, M. O.; Dufresne, E. R. Surface tensiometry of phase separated protein and polymer droplets by the sessile drop method. *Soft Matter* **2021**, *17*, 1655–1662.
- (72) Broedersz, C. P.; MacKintosh, F. C. Modeling semiflexible polymer networks. *Rev. Mod. Phys.* **2014**, *86*, 995.
- (73) Coussot, P. Yield stress fluid flows: A review of experimental data. *J. Non-Newtonian Fluid Mech.* **2014**, *211*, 31–49.
- (74) Camelin, I.; Lacroix, C.; Paquin, C.; Prevost, H.; Cachon, R.; Divies, C. Effect of chelating agents on gellan gel rheological properties and setting temperature for immobilization of living bifidobacteria. *Biotechnol. Prog.* **1993**, *9*, 291–297.
- (75) Makadia, H. K.; Siegel, S. J. Poly Lactic-co-Glycolic Acid (PLGA) as Biodegradable Controlled Drug Delivery Carrier. *Polymers* **2011**, *3*, 1377–1397.
- (76) Pusey, P. N.; Van Meegen, W. Phase behaviour of concentrated suspensions of nearly hard colloidal spheres. *Nature* **1986**, *320*, 340–342.
- (77) Manoharan, V. N. Colloidal matter: Packing, geometry, and entropy. *Science* **2015**, *349*, 1253–751.
- (78) Sicher, A.; Ganz, R.; Menzel, A.; Messmer, D.; Panzarasa, G.; Feofilova, M.; Prum, R.; Style, R.; Saranathan, V.; Rossi, R. M.; et al. Structural Color from Solid-State Polymerization-Induced Phase Separation. *Soft Matter* **2021**, *17*, 5772.
- (79) Wei, M.; Gao, Y.; Li, X.; Serpe, M. J. Stimuli-responsive polymers and their applications. *Polym. Chem.* **2017**, *8*, 127–143.